PAPER • OPEN ACCESS

Preliminary design and performance analysis of a positive displacement hydraulic turbine

View the article online for updates and enhancements.

Preliminary design and performance analysis of a positive displacement hydraulic turbine

Arihant Sonawat[1,2]**, Seung-Jun Kim**[1,2]**, Young-Seok Choi**[1,2]**, Kyoung-Yong Lee**[2]**, Kyung Min Kim**[3]**, Yong-Kab Lee**[4] **and Jin-Hyuk Kim**[1,2]

[1] Advanced Energy & Technology, University of Science and Technology, Daejeon 34113, Republic of Korea
[2] Thermal & Fluid System R&D group, Korea Institute of Industrial Technology, Cheonan 31056, Republic of Korea
[3] Frontier Research & Training Institute, Korea District Heating Corporation, Gyeonggi-do 17099, Republic of Korea
[4] Anflux Co., Ltd., Seoul 08378, Republic of Korea

jinhyuk@kitech.re.kr

Abstract. Positive displacement turbines (PDT) find their use in applications with low flowrate, high head and having lower specific speed requirement, which is below the operational range of the conventional turbines. In the present work, an initial PDT was designed using the governing equations of fluid flow to extract the unused energy from the hot water transportation pipelines. The turbine was of lobe type with two rotors each having four lobes. The tip clearance, side clearance and other leakage losses were considered while designing using fundamental principles coupled with the empirical co-relations from the literature. The initial design's performance analysis had been carried out numerically using commercial computational fluid dynamics (CFD) code ANSYS CFX. The objective of the present study was to reveal the performance of the preliminary design for the given conditions and examine the causes of pulsations in torque, pressure and flow rate from the fluid flow characteristics.

1. Introduction

The dependence of the world on power has greatly increased with the rapid industrialization and increase in ease of life of people. Power shortage can be a major hindrance to a country's growth, development and prosperity. The greater dependence on fossil fuels to fulfill the power requirements has led to serious environmental issues like pollution, global warming, etc. This has paved way for finding alternate energy and power sources which are clean. One such source is hydro power which is renewable. The process of harnessing the potential energy of the flowing water into mechanical or electrical energy is known as hydro power and the systems are known as hydro power systems or plants [1-4]. These systems are classified as micro hydro power systems when the power generation capacity is up to 100kW [5]. Such type of systems assume prominence in places which are not connected with the electrical supply grids, generating power from unconventional sources like sewage systems or in the present case tapping the unused power from the hot water transportation pipelines.

The key component for any hydro power system is the turbine, which is responsible for tapping the hydro power. The overall cost of the system will increase and its efficiency will decrease if a higher

rating turbine is used for low power generation [6]. Hence, attention must be focused on selecting a particular type of turbine for a specific application. This selection depends on the site characteristics, most important of them being the available head, flow rate and specific speed [7-8]. Turbines are broadly classified as impulse turbines (Pelton, Turgo and Cross flow) and reaction turbines (Francis, Kaplan and Propeller) based on the method of generating power. The specific speed (N_s) is given by

$$N_s = \frac{NP^{1/2}}{H^{5/4}}$$ (1)

where, rotational speed (*N*) is in rev/min, power (*P*) in kW and head (*H*) in m. The Pelton turbine is preferred for applications having specific speed in the range of 10-50, Francis turbine works best for specific speed range 50-250 and Kaplan turbine in the range 250-850 [6-8]. In the present study an effort has been made to tap the hydro power potential of the hot water supply system. The average specific speed range for this system is around 6.1, which is beyond the efficient operating capacities of the conventional hydro turbines. Hence a new class of turbine known as Positive Displacement Turbine (PDT) has been developed. The use of this class of turbine has been proposed by Phommachanh et al. [8] and Kurokawa et al. [9].

In the present work, a CFD analysis was undertaken for the designed PDT to evaluate its performance for the given conditions and to get the detailed insight of the fluid flow characteristics. This can aid in rectifying the shortcomings in the initial design and pave way for optimizing the initial design to get the best performance. The adopted numerical technique and the obtained results are discussed subsequently.

2. Numerical Modeling Approach

With the development in high speed computing facilities and reliable and robust mathematical models and codes, computational fluid dynamics (CFD) has attained an integral part in modern problem solving techniques. CFD codes and tools finds their applications in many industries like aerospace, ship building, turbomachines, marine engineering, oil and gas, automobiles, etc. The inherent advantage of using these tools is to find quick and reliable solution for an existing problem economically. Also detailed insight into fluid flow characteristics can be obtained to better analyze the minutes of the problem.

The preliminary design was based on the specified differential pressure, head, flow rate and considering the theoretical and empirical co-relations for various losses like the tip clearance and leakage. The rotors of turbine were lobe shaped. The turbine consisted of two rotors rotating in opposite direction to each other. Both the rotors were identical and each having four lobes. A minimum and uniform clearance of 0.15 mm was maintained between both rotors and between the rotors and casing to satisfy the manufacturing constraint. The key dimensions of the initial design are listed in table 1, non-dimensionalised by the inlet pipe diameter.

Any CFD study starts with the initial step of creating a geometrical model of the design. In the present study, a three-dimensional (3-D) model of the PDT was created in SOLIDWORKS® as shown in figure 1. The model was designed based the methodology from Zhaohui and Smith [10]. Special attention was paid that the rotors while rotating do not overlap with each other at any point. Also the inlet and outlet pipe length was kept at 10 times the rotor diameter so as to have uniform and undisturbed fluid flow free from any property changes or phenomenon happening at the rotors. The fluid domain was meshed with structured hexahedral grids. The advantage of using structured grid is to obtain an accurate and reliable solution with small computation time and resource [11]. Fine grids were generated in the regions prone to change in fluid characteristics and flow phenomenon like the near wall regions, the clearance region, rotor-rotor interface, rotor-stator interface, etc. as shown in figure 2. A grid independency study was performed to ensure that obtained solutions do not change

Table 1. Key dimensions for the preliminary design of PDT.

S.No	Parameters	Value
1	Rotor diameter ratio	1.3409
2	$t_c=r_c=s_c$	0.15 mm
3	Rotor width ratio	1.03409
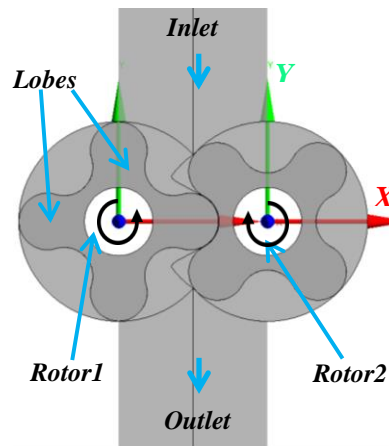
Figure 1. 3-D model of the PDT.
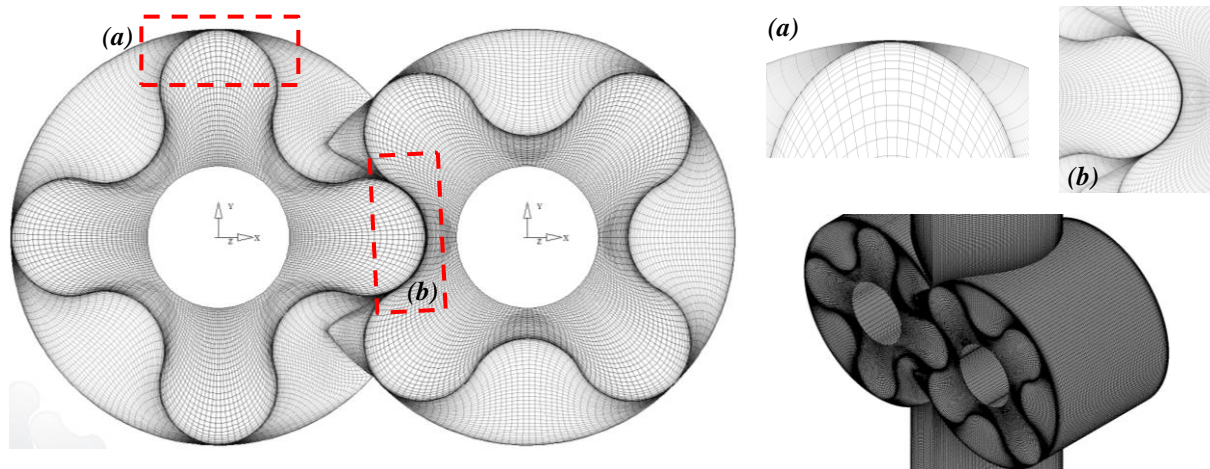
Figure 2. View of mesh.

with the grid size as shown in figure 3. It can be seen from figure 3 that the pressure ratio (P_R), flow ratio (Q_R) and torque ratio (T_R) became invariant with the increase in grid size beyond 1.3 million nodes. Hence, for further calculations, grid with 1.3 million nodes node was used.

The governing equations of the fluid flow like the continuity and momentum were solved by an unsteady approach using CFD tool ANSYS CFX v17.1. The turbulence effects of the fluid flow were evaluated using $k - \omega$ Shear Stress Transport (SST) model which gives reasonably accurate results for such type of problems [12-13]. The advection terms in the governing equations were discretized using high resolution scheme, second order backward Euler scheme was incorporated for transient terms and first order scheme was used for turbulence numeric. In order to capture accurately the complex nature of flow, moving mesh was used. The mesh was deformed for every 1° rotation of the rotors using
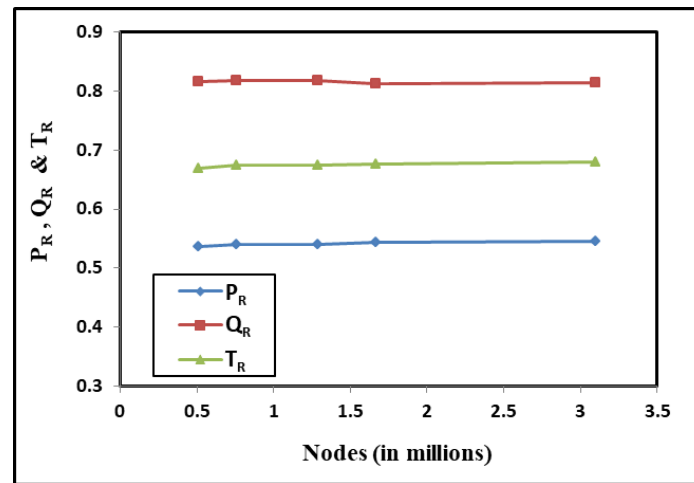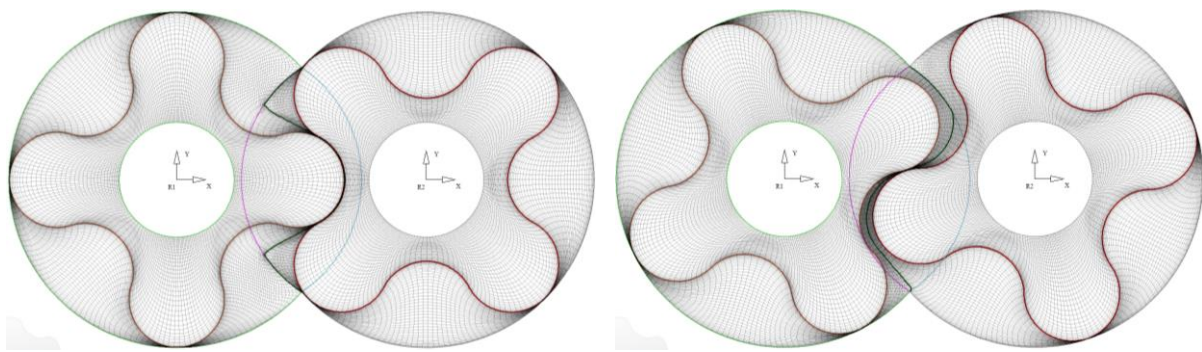
Figure 3. Grid independency study.

Figure 4. Mesh deformation.

Table 2. Operating conditions.

S.No	Parameters	Value
1	Working fluid	Water
2	Head Coefficient at inlet (H_{cin})	320.706
3	Head Coefficient at outlet (H_{cout})	96.036
4	Rotational Speed Coefficient (N_c)	0.05584
5	Temperature	110 °c

FORTRAN subroutines provided by the meshing tool TWINMESH® as shown in figure 4. The following assumptions were considered while solving the governing equations. The fluid was assumed to be incompressible. The wall was assumed to be smooth and adiabatic.

The inlet and outlet were assigned as pressure inlet and outlet boundary conditions. A no-slip boundary condition was specified at the walls. In order to achieve a reliable and converged solution, the governing equations were iterated until the residuals of the dependent variables dropped below 10^{-3} and a mass imbalance of 0.01 was satisfied. In the present case, the root mean square (RMS) residuals of the continuity and momentum terms attained a quasi-steady state after two loop rotation of the rotors. The simulations were stopped after two rotors revolutions (i.e, 8 loop rotations). Table 2 gives the details of the incorporated boundary conditions. The head coefficient (H_c) is given by

$$H_c = \frac{gH}{(nD)^2} \tag{2}$$

where, g is the acceleration due to gravity ($g = 9.81$ ms^{-2}), n is the rotational speed in rev/s and D is the rotor diameter. The rotational speed coefficient (N_c) is expressed as
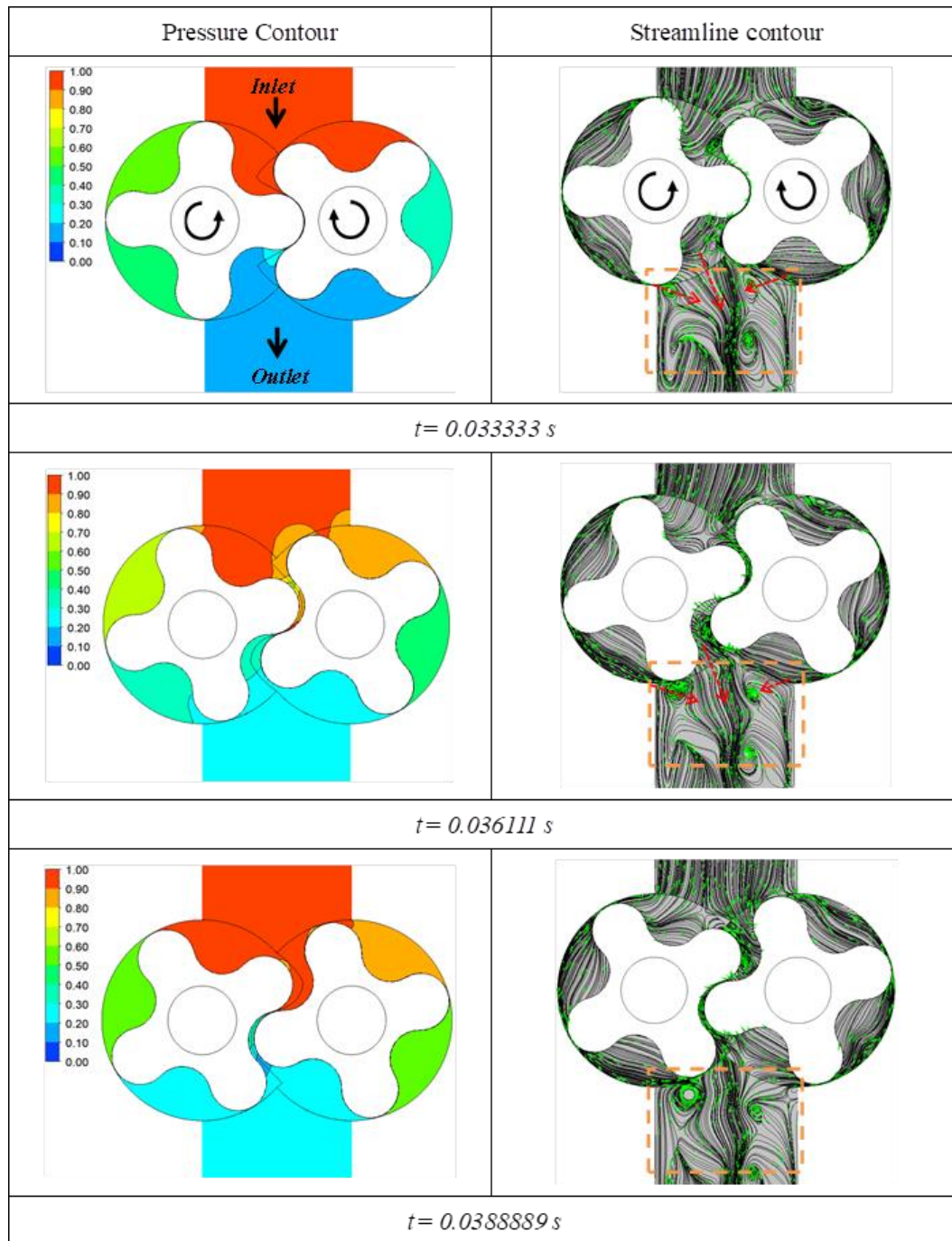
$$N_c = \frac{nD}{(gH)^{0.5}} \tag{3}$$

Figure 5. Fluid flow characteristics at different instants of time.

3. Results & Discussion

A relatively uniform flow, which is at high pressure and temperature, enters the rotors through the inlet pipe. The pressure at the outlet is lower than the inlet and due to this differential pressure (ΔP), the fluid causes the rotors to rotate. As it can be seen from the pressure contours in figure 5, the pressure at the inlet void between the lobes of the rotors is high and the pressure in the subsequent void is comparatively lower. This differential pressure results in the rotation of the rotors. Both the rotors rotate independently under the influence of the existing differential pressure. The rotor 1 rotates in the counter-clockwise direction while the rotor 2 rotates in the clockwise direction. A recirculation zone is formed near the casing of the rotors. This is due to the mixing of the high velocity low pressure fluid leaking through the clearance between the rotor and the casing, and comparatively high pressure and low velocity fluid present between the voids of the lobes. The flow leaving the rotors to the outlet pipe is very chaotic and recirculating. This is due to the mixing of the high velocity leakage fluid leaving the clearances (gap between rotors and casing and gap between both the rotors) and low velocity uniform form flow leaving the voids. Large vortices and irregularities result due to the mixing of the leakage flow with the main bulk of flow as seen in the streamline contours of figure 5.
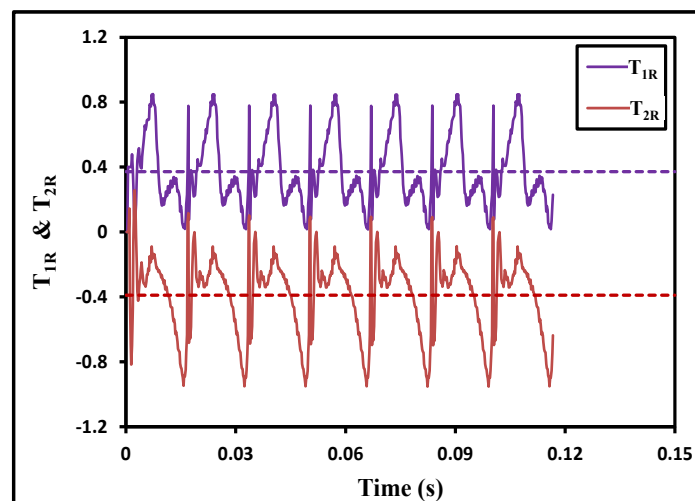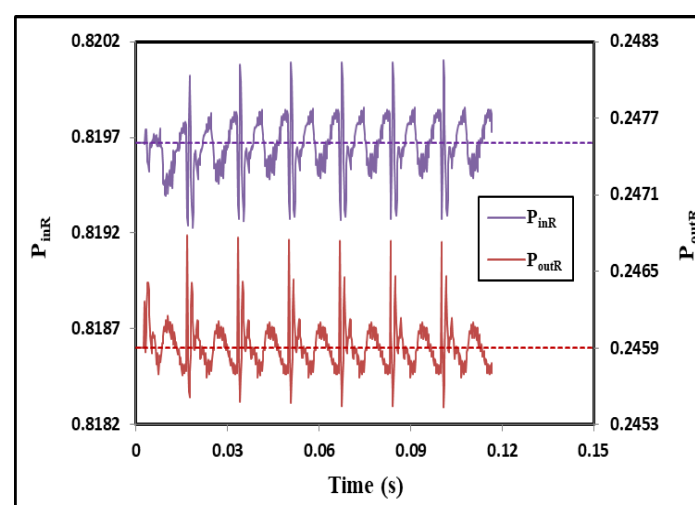

Figure 6. Variation of torque.

Figure 7. Pressure fluctuations at inlet and outlet.

Figure 6 shows the variation of the torque at both the rotors with time. T_{1R} and T_{2R} are the torque ratios at rotor 1 and rotor 2 respectively, where $T_{1R} = T_1 / T_{max}$ and $T_{2R} = T_2 / T_{max}$. Here T_1 and T_2 are the instantaneous torque values at rotor1 and 2 respectively and T_{max} is the ensemble averaged maximum total torque. The reason for this fluctuation is the continuous change in the contact area (void between lobes) seen by the incoming and discharge flow due to the rotation of the rotors. At some inlet locations, the inlet flow sees the entire void space. Hence large volume of fluid can enter that rotor. Greater is the amount of high pressure fluid entering the voids, greater will be the force exerted on the rotors to rotate and hence the resultant torque will also be higher. The converse of this is also true. Also, it can be noted from the figure 5, the incoming and the outgoing flow from both the rotors is subjected to different contact areas at every instant of time. Hence, resulting in the fluctuation of inlet and outlet pressure (as shown in figure 7) and torque (as shown in figure 6), where $P_{inR} = P_{in} / P_{max}$ and $P_{outR} = P_{out} / P_{max}$. Here P_{inR} and P_{outR} are the inlet and outlet pressure ratios, P_{in} and P_{out} are the instantaneous pressures at the inlet and outlet respectively and P_{max} is the ensemble averaged maximum pressure in the domain.
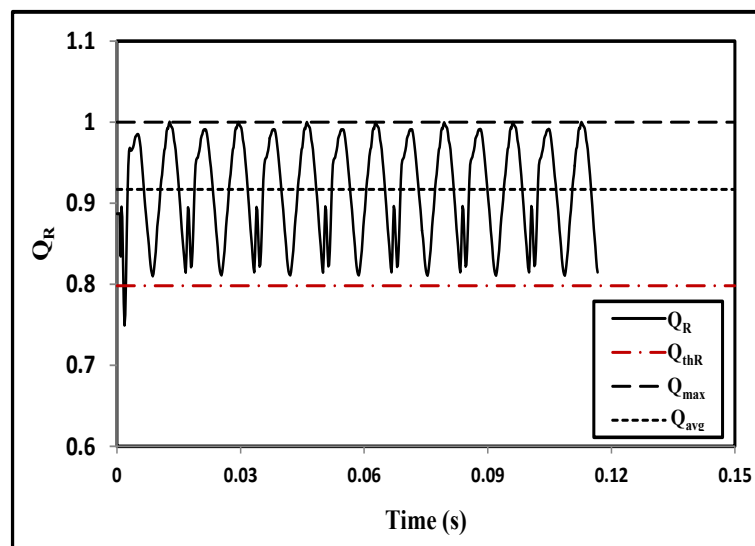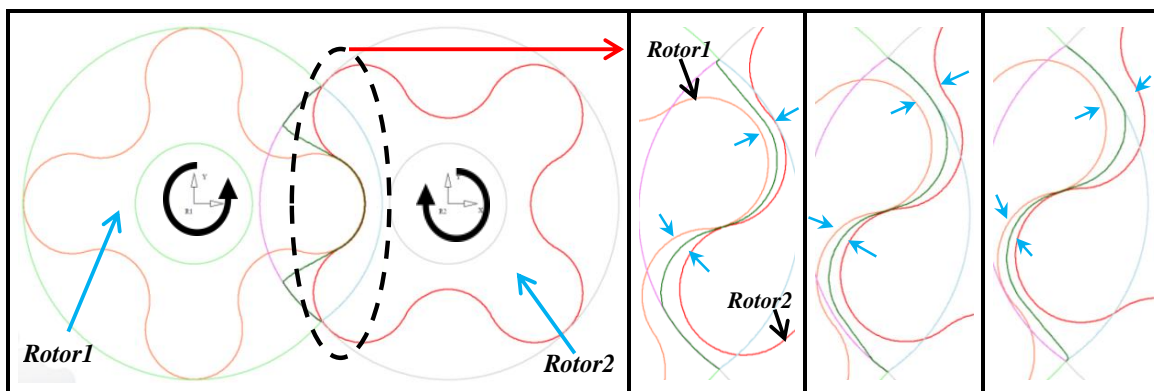

Figure 8. Variation of flowrate and validation.

Figure 9. Variation of r_c with the rotation of rotors.

29th IAHR Symposium on Hydraulic Machinery and Systems

IOP Conf. Series: Earth and Environmental Science **240** (2019) 022009

IOP Publishing

doi:10.1088/1755-1315/240/2/022009

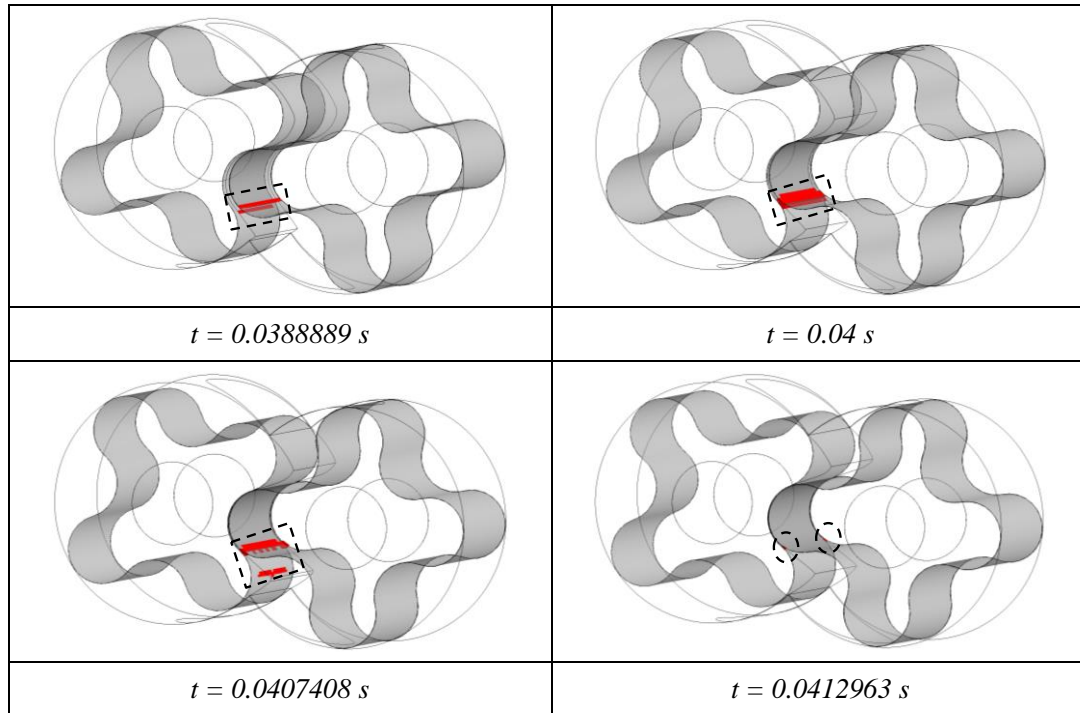|	
t = 0.0388889 s	*t = 0.04 s*
t = 0.0407408 s	*t = 0.0412963 s*

Figure 10. Occurance of cavitation regions.

Figure 8, shows the variation of the calculated volumetric flowrate (Q) at every instant of time expressed non-dimensionally in terms of flow ratio (Q_R), where $Q_R = Q / Q_{max}$. Here Q is the instantaneous flow rate through the domain, Q_{max} is the ensemble averaged maximum flowrate and Q_{avg} is the ensemble averaged mean flowrate. The flowrate ratio keeps fluctuating between maximum and minimum values with time. This is compared with the theoretical flowrate ratio (Q_{thR}) which is calculated by $Q_{thR} = Q_{th} / Q_{max}$ and

$$Q_{th} = V_d \times N \qquad (4)$$

where V_d is the displacement volume (volume of the fluid which occupies the rotor voids) and Q_{th} is the calculated theoretical flow rate. A satisfactory agreement is achieved between both the results showing the validness of the CFD methodology. The theoretical flowrate is calculated with the assumption that there exists no clearance between the rotors and between the rotors and casing. Hence there is no leakage flow. Practically, due to manufacturing constraints, to avoid rotor-rotor overlap and to avoid shear between rotors and casing, a constant clearance of 0.15 mm is considered, i.e, tip clearance between rotors and casing (t_c) and clearance between both the rotors (r_c) and clearance between rotors and side walls (s_c) is 0.15 mm. This will result in flow losses due to leakage of fluid through them. The leakage flow flowrate is approximately 5-20% of the theoretical flowrate. The leakage losses will be higher at higher rotational speeds and greater clearance [8-9]. It is very interesting to note that although a constant clearance is provided between both the rotors initially, but due to the rotation of both the rotors in opposite direction, the resulting actual clearance between them is not constant, but varying at every instant of time due to change in the relative lobe positions as shown in figure 9. This results in greater leakage losses through this area and subsequently fluctuation in the flowrate. Also the variation in the r_c results in the generation of very low pressure regions in that area. The resulting pressure is lower than the saturation pressure of the fluid at that temperature and thus causes the formation of cavitation zones. The fluid present between these regions is squeezed out abruptly due to contraction in volume arising from the rotation of the rotors. Thereby, resulting in the

formation of cavitation zones. In the present case, the cavitation region is very narrow and its occurrence is limited to few instants when there is sudden contraction of volume. It can be seen from figure 10, at time t=0.0388889 s, due to contraction of the clearance volume, there is onset of cavitation which increases with the contraction and finally it is eliminated as the clearance volume is expanded at time t = 0.0412963 s. The occurrence of cavitation is not a desirable phenomenon in any turbomachinery as it results in performance and structural losses. Since the cavitation zone in the present case is restricted to a very narrow region of the entire turbine and its occurrence is limited to some particular instants of time, hence its effect is not considered very significant and catastrophic. Further research is underway to completely eliminate this phenomenon and hence not included as the scope of this article.

The performance of the developed initial PDT is expressed in terms of characteristics like torque ratio (T_R), power ratio (P_R), flowrate ratio (Q_R) and effective head ratio (H_{ER}) etc. The torque ratio is defined as

$$T_R = \frac{T}{T_{max}} \tag{5}$$

where, T is the ensemble averaged total torque from both the rotors and T_{max} is the observed ensemble averaged maximum torque. The power ratio which is analogous to the hydraulic efficiency is the ratio of time averaged output power to the input power expressed as

$$P_R = \frac{P_{output}}{P_{input}} = \frac{T.n}{\Delta P.Q_{avg}} \tag{6}$$

The effective head ratio is defined as the ratio of difference between inlet and outlet head to that of inlet head and is expressed as

$$H_{ER} = \frac{H_{in} - H_{out}}{H_{in}} = \frac{H_E}{H_{in}} \tag{7}$$

where, H_{in} & H_{out} are the heads at inlet and outlet respectively. H_E is the effective head which is the difference between the inlet head (H_{in}) and the outlet head (H_{out}).

Figure 11 shows the performance curves of the developed PDT against the effective head ratio at constant rotational speed. For a constant inlet pressure, a high effective head means lower discharge
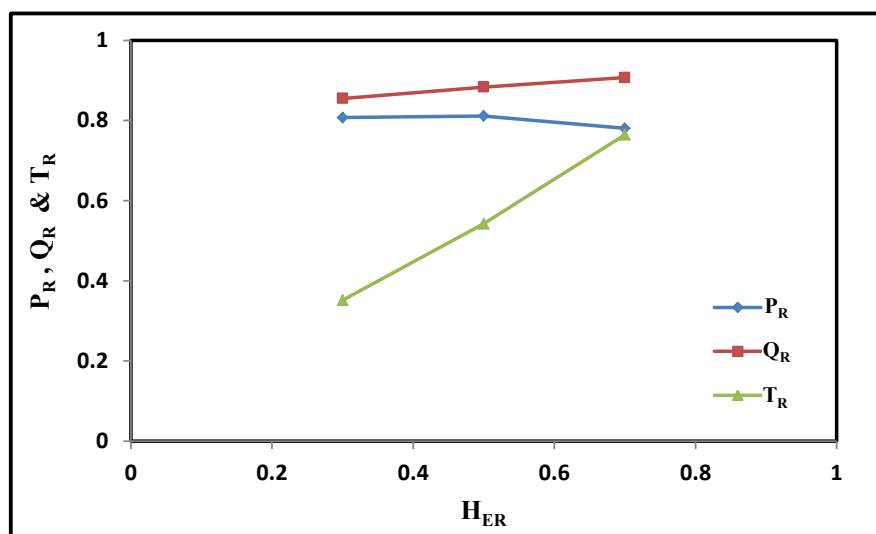

Figure 11. Performance of PDT.

pressure and vice versa. At low effective head, the energy in the fluid available for the turbine to expand is low. Hence, the torque and subsequently the output power are low. With an increase in effective head, the available energy increases permitting the fluid to expand at lower discharge pressure. This result in enhanced torque and output power which is expressed non-dimensionally in terms of torque ratio and power ratio in figure 11. The dependence of torque and output power on effective head is higher than flowrate. The variation in flowrate is influenced by the rotational speed.

4. Conclusions

A positive displacement turbine was designed for the specified operating conditions using the fundamental principles. The application of this PDT was for harnessing the untapped energy from the water transportation pipelines, which is otherwise dissipated. The unsteady numerical analysis of the preliminary design revealed the pulsating nature of flow. The causes of these pulsations were examined from the fluid flow characteristics. The pulsation in torque and pressure was due to the continuous change in void area seen by the fluid and the pulsation in flowrate was due to the increased leakage losses arising from squeezing of fluid from the variation in the clearance volume. The drop in the overall hydraulic performance was the result of leakage losses and flow irregularities arising from the mixing of leakage flow with the main flow. Also, the occurrence of cavitation was identified and elimination of it will be performed.

Acknowledgment

References

[1]   Nasir B A 2013 Design of micro-hydro-electric power station *International Journal of Engineering and Advanced Technology*. **2** 39

[2]   Varughese A and Michael P A 2013 Electrical characteristics of micro-hydro power plant proposed in valara waterfall *International Journal of Innovative Technology and Exploring Engineering, IJITEE*. **2**

[3]   Archetti R 2011 Micro hydroelectric power: feasibility of a domestic plant *Procedia Engineering*. **21** 8

[4]   Yannopoulos S I, Lyberatos G, Theodossiou N, Li W, Valipour M, Tamburrino A and Angelakis A N 2015 Evolution of water lifting devices (pumps) over the centuries worldwide *Water*. **7** 5031

[5]   Khurana S, and Kumar A 2011 A Small hydro power—A review International Journal of Thermal Technologies. **1** 107

[6]   Jawahar C P and Michael P A 2017 A review on turbines for micro hydro power plant *Renewable and Sustainable Energy Reviews*. **72** 882

[7]   Zainuddin H, Khamis A, Yahaya M S, Basar M F M, Lazi J M and Ibrahim Z 2009 Investigation on the performance of pico-hydro generation system using consuming water distributed to houses *Proceedings of the developments in renewable energy technology*.

[8]   Phommachanh D, Kurokawa J, Choi Y D and Nakajima N 2006 Development of a positive displacement micro-hydro turbine *JSME International Journal Series B Fluids and Thermal Engineering*. **49** 482

[9]   Kurokawa J, Matsui J and Choi Y D 2008 Flow Analysis in Positive Displacement Micro-Hydro Turbine and Development of Low Pulsation Turbine *International Journal of Fluid Machinery and Systems*. **1** 76

[10]   Zhaohui Y Z and Smith M R 2004 Design and cutting of three-lobe helical rotor in roots blower *Chinese Journal of Mechanical Engineering*. **20** 17(Supplement):1

[11]   Hirsch C 2007 Numerical computation of internal and external flows. Oxford, Great Britain.

John Wiley & Sons, Ltd

[12]   YU X B and ZHEN H X 2007 Comparison of RNG k-ε and SST k-ω Turbulence Model for Computation of Complex Flow Field around Automobile [J] *Auto Mobile Science & Technology*. **6** 011

[13]   Sonawat A, Choi Y S, Lee K Y, Yang H M and Kim J H 2017 Feasibility Analysis of Existing Compressor Design for Different Refrigerants *International Journal of Fluid Machinery and Systems*. **10** 336